Implementation of a New Algorithm to Detect Turn-to-Turn Faults in Shunt Reactors and Identify the Faulted Phase

Paul I Nyombi
Xcel Energy
Minneapolis, MN

Zhiying Zhang
General Electric Grid Solutions
Canada

Pratap G Mysore
Pratap Consulting Services, LLC
Plymouth, MN

Abstract— Detection of the turn-to-turn fault in shunt reactors has been a challenging task for P&C engineers. This is because turn-to-turn faults create very small changes in the currents and voltages that the relay measures, where existing methods don't have enough sensitivity to detect such faults. Undetected failure will result in loss of the entire reactor phase. Recently, a new algorithm, allowing for much better sensitivity, was proposed providing a reliable way to detect turn-to-turn faults and reliably identify the faulted phases [3]. The new algorithm makes use of the negative sequence and the positive sequence voltage and current measurements to develop a differential scheme to sensitively detect shunt reactor internal faults.

With the advantage of expanded programming capabilities in modern relays, Xcel Energy was able to program this algorithm and successfully test it by playing back records captured during several shunt reactor failure events. The new algorithm was able to identify the turn-to-turn faults and the faulted phases simultaneously, for all the events indicating the superiority of this algorithm over the existing techniques. The algorithm remained stable for several cases of shunt reactor energization and external faults. The algorithm has been deployed in the field for evaluation.

This paper will present Xcel Energy's approach to achieve better shunt reactor protection utilizing this algorithm and share their findings.

***Index Terms*—Shunt Reactors, Turn-to-Turn faults, Shunt Reactor Protection**

I. Introduction

Xcel Energy has several shunt reactors installed to control system voltages to within the acceptable limits during light load conditions. The reactors are installed on transmission transformers' tertiaries, buses, and on transmission lines. Shunt reactors installed on transformer tertiaries and bus positions are of air core type. In the recent years, an increasing number of shunt reactors, particularly those installed on 34.5kV transformer tertiaries, have been failing. This called for re-evaluation of the switching transients' mitigation methods and protection schemes. Protection of air core reactors, especially as regards turn-to-turn faults, will be the main focus of this paper's discussion. Even though, oil-immersed reactors aren't specifically considered in this paper, the same protection principles discussed in this paper do equally apply to them and a case or two will be considered.

1.1. Turn to Turn Fault Protection Schemes

Detection methods discussed in the IEEE guide for protection of Shunt Reactors [1] utilize negative sequence overcurrent and directional methods on any reactor configuration and voltage unbalance relaying on ungrounded reactors.

Negative sequence overcurrent protection has to be set above inherent unbalances and has to be coordinated with other protection schemes for faults external to the reactor thus providing a slow protection scheme.

Negative-sequence directional element (32Q) can provide a secure and very sensitive protection to detect unbalances caused by turn to turn fault within the reactor [2].

Voltage differential schemes employed on ungrounded wye configured reactors connected to transformer tertiaries compare the reactor neutral voltage with the 3V0 on the phase terminals.

It is to be noted that none of these methods can identify the faulted phase without further analysis.

II. New proposed Method

Relay algorithm proposed in the published paper [3] looks at the relationship between the negative sequence voltages and currents.

This algorithm operates on the difference between the negative sequence normalized voltage *(1)* and negative sequence normalized current *(2)*. *Figure 1* will be used for illustration.

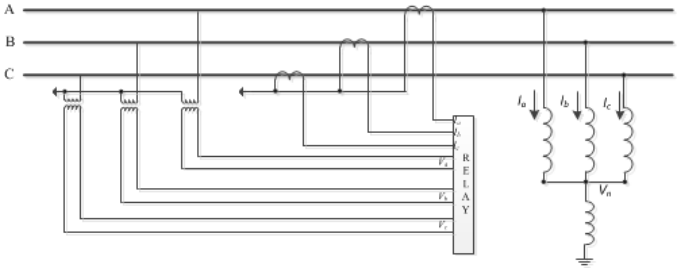

Figure 1: Wye-Connected Shunt Reactor

The principle of operation of this algorithm is briefly explained below:

Negative sequence voltage normalization is given as:

$$\frac{V_2}{V_1} = \frac{V_a + a^2 V_b + a V_c}{V_a + a V_b + a^2 V_c} \quad (1)$$

Where the *operator a* is define as $1e^{120^\circ i}$

Negative sequence current normalization is given as:

$$\frac{I_2}{I_1} = \frac{I_a + a^2 I_b + a I_c}{I_a + a I_b + a^2 I_c} \quad (2)$$

Consider Z_a, Z_b, & Z_c phases to be reactor impedances for A, B, and C-Phases respectively.

$$\frac{I_2}{I_1} = \frac{\frac{V_a - V_n}{Z_a} + a^2\frac{V_b - V_n}{Z_b} + a\frac{V_c - V_n}{Z_c}}{\frac{V_a - V_n}{Z_a} + a\frac{V_b - V_n}{Z_b} + a^2\frac{V_c - V_n}{Z_c}} \quad (3)$$

Where,V_n, as shown in *figure 1*, is zero for solidly grounded reactors.

For $Z_a = Z_b = Z_c = Z$,

$$\frac{I_2}{I_1} = \frac{V_a + a^2 V_b + a V_c - (V_n + a^2 V_n + \alpha a)}{V_a + a V_b + a^2 V_c - (V_n + a V_n + a^2 V_n)} \quad (4)$$

$$\frac{I_2}{I_1} = \frac{V_a + a^2 V_b + a V_c}{V_a + a V_b + a^2 V_c} \quad (5)$$

Combining *equations (1)* and *(5)*, gives $\frac{V_2}{V_1} = \frac{I_2}{I_1}$.
Note that this equation is valid for all balanced or unbalanced system voltages as long as all reactor impedances are equal or nearly equal. During turn-to-turn faults, the faulty phase impedance changes, and leads to $\frac{V_2}{V_1} \neq \frac{I_2}{I_1}$.

The phasor difference between these two values ($\frac{V_2}{V_1}$ and $\frac{I_2}{I_1}$) will be used to compute the operating quantity in detection of turn-to-turn faults in shunt reactors.

The phasor angle associated with the operating quantity is used to identify the faulted phase, which makes it superior over other algorithms. This is selected as per *table 1* [3].

$Diffangle$	*Phase selection decision*
$150^o \leq Diffangle \leq 210^o$	*Turn to turn fault in phase A*
$270^o \leq Diffangle \leq 330^o$	*Turn to turn fault in phase B*
$30^o \leq Diffangle \leq 90^o$	*Turn to turn fault in phase C*

Table 1: *Operating quantity* phasor angle for identifying the faulted reactor phase

The algorithm is discussed in detail in [3]. This paper will only focus on its practical application and field implementation.

III. IMPLEMENTATION OF NEW ALGORITHIM

A. Setting Philosophy

Maximum normal voltage imbalance of 10% is considered in determining the tolerance on $V_{Neg\_Normalized}$ $\left(\frac{V_2}{V_1}\right)$ and $I_{Neg\_Normailized}$ $\left(\frac{I_2}{I_1}\right)$. If the maximum expected PT and CT measurement errors are $\pm 5\%$ of the measured values, the worst expected steady state difference, Diff$steady$, will be given as:

$$\%\, V_{Neg\_Normalized} = 10 \text{ x } 1.05 = 10.5\% \quad (6)$$
$$\%\, I_{Neg\_Normailized} = 10 \text{ x } 0.95 = 9.5\% \quad (7)$$

$$\%\text{Diff}steady = 100\left(\frac{V_2}{V_1} - \frac{I_2}{I_1}\right) = |10.5 - 9.5| = 1.0\% \quad (8)$$

The differential pickup value, Diff$pickup$, must be set higher than 1.0%. As per the IEEE Std C57.21-2008 [4], the maximum deviation of impedance in any of the phases shall be within $\pm 2.0\%$ of the average impedance of the three phases. For all practical purposes, Diff$steady$, as computed above should be sufficient.

To protect the reactor, Diff$pickup$ is set to pick up for at least 5% reduction in the reactor winding impedances.

Suppose the B-Phase reactor starts failing with 5% decrement its winding impedance, $I_{Neg\_Normailized}$ is computed as:

$$\frac{I_2}{I_1} = \frac{\frac{V_a}{Z_a} + a^2\frac{V_b}{0.95Z_b} + a\frac{V_c}{Z_c}}{\frac{V_a}{Z_a} + a\frac{V_b}{0.95Z_b} + a^2\frac{V_c}{Z_c}} \quad (9)$$

At that fault level, $\frac{V_2}{V_1} \ll \frac{I_2}{I_1}$, and if an infinite source is considered, Diff$pickup$ is calculated as:

$$\text{Diff}pickup = \frac{V_2}{V_1} - \frac{I_2}{I_1} \cong \left|\frac{I_2}{I_1}\right| \times 100 = 1.7\% \quad (10)$$

A practical example with finite source impedance is give in *Annex A* of the appendix to demonstrate that not much accuracy is lost in deriving Diff$pickup$ as given in equation (10).

Due to the assumptions involved in this derivation, a safety factor of 2.0 is applied to both Diff$pickup$, and Diff$steady$.

The *Operate* quantity is therefore, selected so as to be above the normal operating steady state value but below the desired fault pickup level. Pickup value of 2.5% is selected from the range, $2.0\% <$ Diff$pickup$ $< 3.4\%$. Also important to note is that the pickup value is independent of the voltage level and reactor configuration as far as grounding is concerned.

The past, eight (8) real time operating differential values, including the present value are computed and averaged over a power cycle. The averaged differential value, Diff$average$, is compared against the Diff$pickup$.

$$Diff_{average}(n) = \frac{1}{p}\sum_{k=1}^{p=8} Diff_{realtime}(n + 1 - k) \quad (11)$$

B. Logic Implementation

A definite pickup time delay of 240.0 cycles is utilized to momentarily block the algorithm, immediately following shunt reactor energization. This is to ensure that the algorithm is not compromised by CT saturation associated with energization transients. For extra security, a CT saturation word bit, present in some of the modern relays, is also used to further block the scheme upon its assertion– see *figure 2*. The algorithm is also blocked for faults involving the ground. These are detected by presence of substantial zero-sequence voltage. Additionally, the algorithm is only armed if at least 80% of the rated voltage on all three phases is present with the shunt reactor bank in-service.

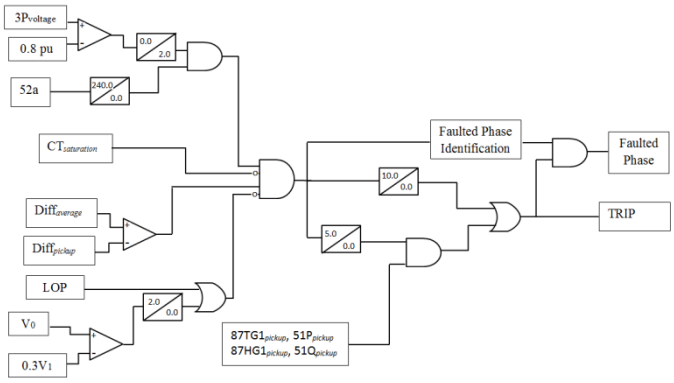

Figure 2: Sensitive turn-to-turn reactor fault detection algorithm

To provide for faster clearing of faults, if any of the other elements picks up while Diff*pickup* is exceeded for at least 5.0 cycles, the 10.0 cycle timer is bypassed and TRIP command is issued right away. The 5.0 cycle delay does ensure that the algorithm performs securely during external disturbances.

Two different relays, presently used by Xcel Energy, have been used to implement the logic discussed above. The relays execute the logic sequentially. They also do run it through the same number of process cycles used for executing fixed critical protection logic. The logic is shown in the appendix under *Annex B.*

IV. CASE STUDIES

A. Ungrounded Tertiary Connected Reactor Failure

Failures associated with a 50 MVAR ungrounded air core reactor, connected to a 34.5kV tertiary of 448MVA 345/115 kV Auto-D transformer, shown in *figure 3*, are considered.

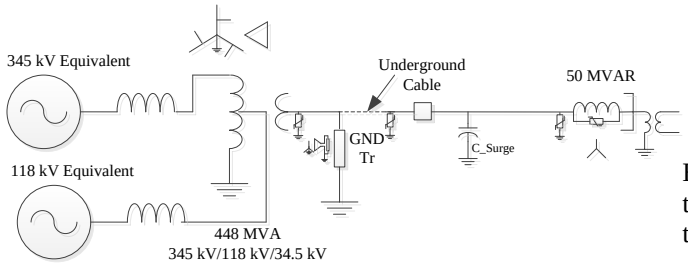

Figure 3: Tertiary Connected Shunt Reactor

Existing protection

The reactor's primary protection comprises two definite time delayed voltage differential elements. The first and more sensitive element (87TG1) is set as shown below:

$$87TG1P = \frac{\frac{\Delta X}{3} \cdot V_{L-n}}{PTR} \quad (12)$$

A maximum of 5.0% reactive impedance deviation from the average reactor impedance is used. A pickup time delay of 5.0s is utilized.

The second voltage element, used for detecting severe reactor faults is set as shown below:

$$87HG1P = \frac{\frac{1}{2} \cdot V_{L-n}}{2 \cdot PTR} \quad (13)$$

A definite 10.0 cycle pickup time delay is used.

Backup protection elements include negative sequence and phase time overcurrent set to pick up at 20% and 135% of the reactor rating respectively. Instantaneous phase over current is also added to the protection scheme to provide backup protection for severe reactor faults.

On 08/26/2017, at 05:43:51, the reactor tripped and locked out. *Figure 4* shows that initial inspection of the reactor revealed charring on the A-Phase reactor.

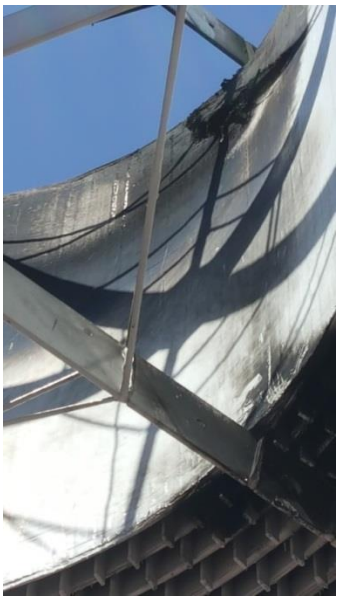

Figure 4: A-Phase faulty reactor following the 8/26/2017 event

Examination of the event records (*figure 5*) revealed that the 87TG1 differential was picked for several cycles before the 87HG1 element picked up and tripped out the reactor.

During the initial phase of the fault, the 51Q, responsible for detecting turn-to-turn reactor faults never detected the fault.

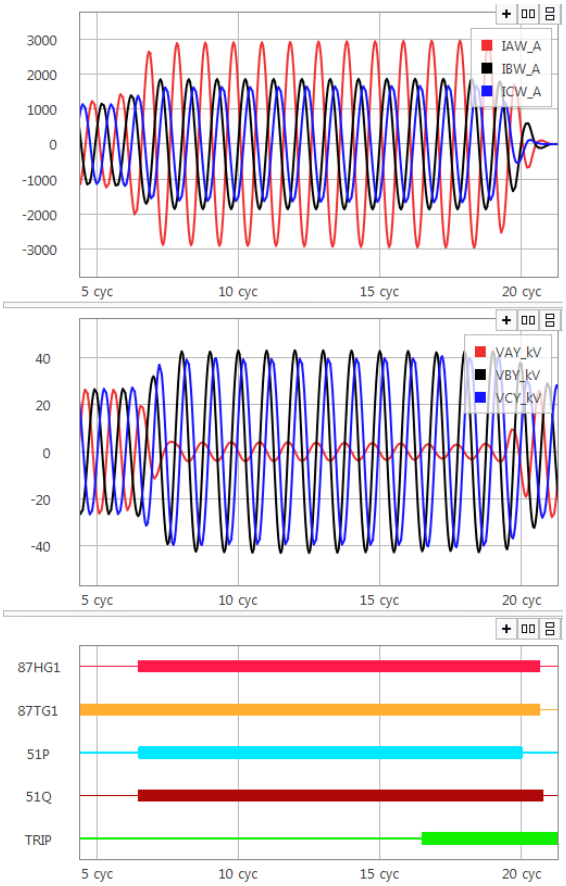

Figure 5: Relay records from the reactor relay following the 8/26/2017 event

Evaluation of the new algorithm

The relay comtrade files where played back in the relay to evaluate the performance of the new algorithm. *Figure 6* shows that the algorithm correctly detects the fault and accurately identifies the faulted phase.

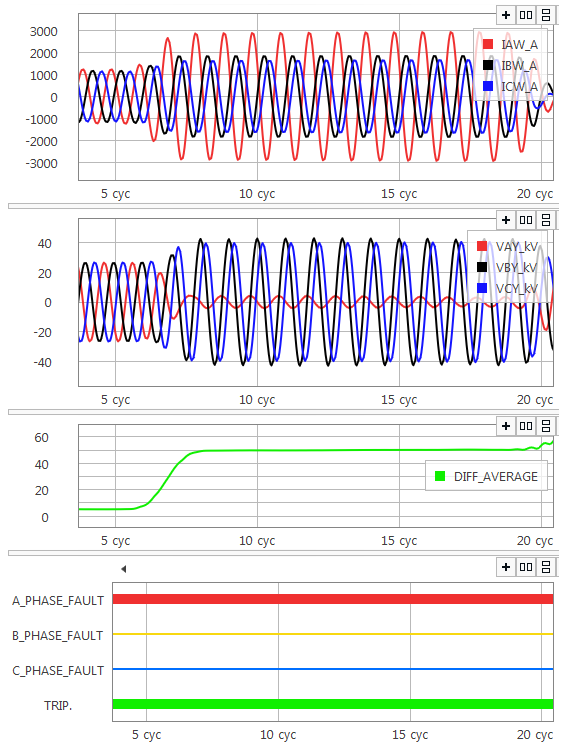

Figure 6: Evaluation of the performance of the new algorithm during the 8/26/2017 event

With a Diff*pickup* setting of 2.5%, it is obvious that the algorithm would have perhaps picked up much earlier than the 87TG1 element did, removing the fault from the system faster. For the portion of the event that was captured, the measured Diff$average$, during the low fault time period is 5.32%. This is more than twice the set Diff*pickup* value. In this same time period, the measured Diff$average$ angle is 198.8 degrees. This fairly matches the, expected ideal theoretical angle value of 180 degrees for turn-turn fault in the A-Phase reactor. It is also important to note that even with severe reactor fault; the algorithm accurately identifies the faulted phase.

The faulted reactor was replaced with a spare reactor and the reactor bank was put back in-service. On 11/12/2017, at 07:37:02, the reactor tripped and locked out again. Field investigation did show that there was visible charring on the C-Phase as shown in *figure 7*.

Figure 7: C-Phase faulty reactor following the 11/12/2017 event

Examination of the event records, shown in *figure 8*, and the sequence of events indicated that the time-delayed voltage differential element picked up for at least 120 cycles before the reactor tripped out.

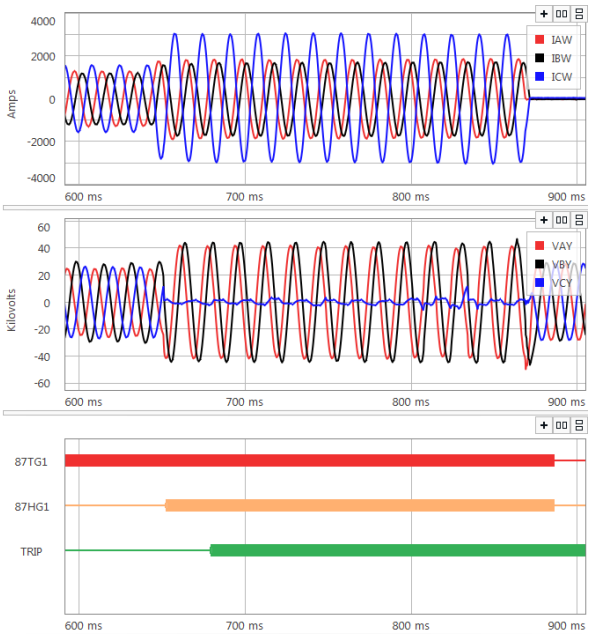

Figure 8: Relay records from the reactor relay following the 11/12/2017 event

The high-set voltage differential element picked up the fault after it severely progressed. By then the fault had been on the system for at least 110 cycles. None of the overcurrent elements detected the fault in the low fault current region.

The comtrade files were played back into the relay to test the algorithm against the new event records. *Figure 9* shows that the algorithm again detects the fault and accurately identifies the faulted phase.

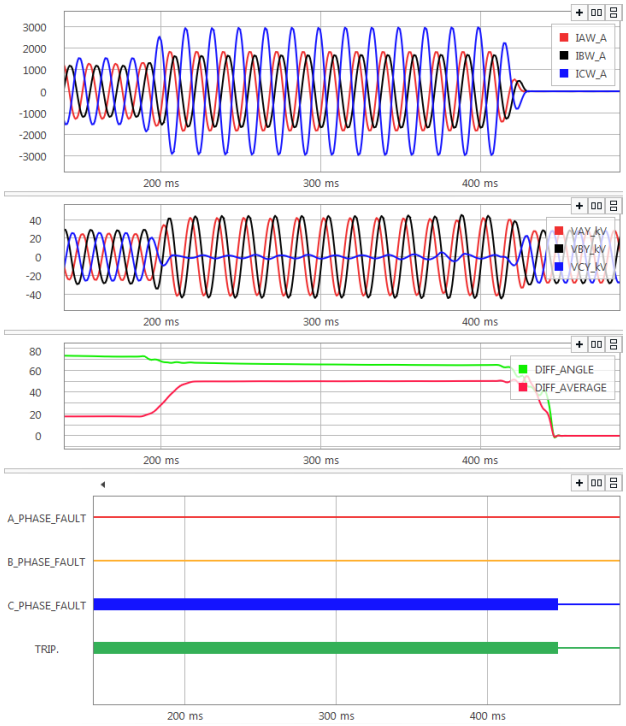

Figure 9: Evaluation of the performance of the new algorithm during the 11/12/2017 event

As was the case with the 8/26/2017 event, it is clear that the algorithm would have sensitively detected the fault and removed it from the system much sooner than the standard protection elements did.

B. Evaluation of the Algorithm against Normal Ungrounded Reactor Energization

Following the two previous reactor failures, all the reactors were scrapped and replaced with new ones. The performance of the new algorithm was evaluated against transients associated with reactor energization. It was observed that for the energization transients considered the algorithm remained secure. However, when the algorithm was deployed in the field, for evaluation at a different but similar reactor installation (with an overhead bus instead of cable), for some switching transients, it was observed that the initial thirty cycles delay that was suggested for blocking the algorithm following energization was not adequate. The algorithm was initially successfully blocked for the first thirty cycles as expected. *Figure 10* shows current energization transients. The calculated Diff*average* jumped up well above the Diff*pickup* setting as soon as the timer dropped out and remained high for a significant number of cycles. *Figure 11,* shows Diff*average* nearly a hundred (100) cycles after the shunt reactor energization. The differential value is seen to slowly decrease, almost linearly, until it reaches its final relay calculated steady state value of about 0.2%.

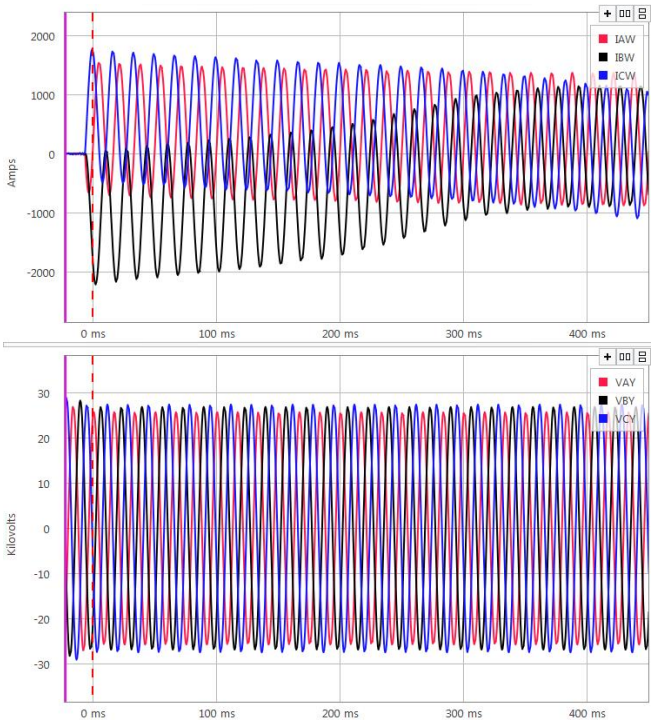

Figure 10: Field evaluation: Shunt reactor energization current transients

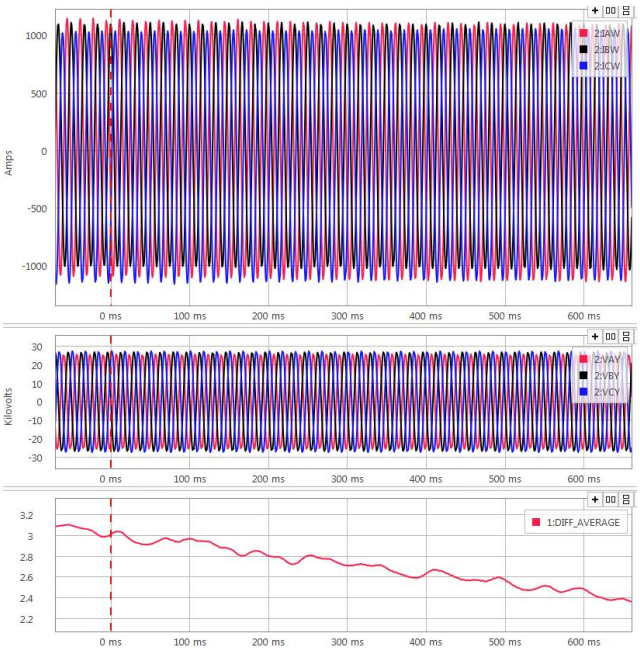

Figure 11: Field evaluation: Shunt reactor current transients, 100 cycles after energization

Observations from this particular event seem to indicate that the sudden loss of DC by at least one of the reactor currents (B-Phase in this case) leads to the incorrect transformation of primary currents as explained in Reference [4]. The uneven saturation of the CTs, which varies with the reactor breaker closing angles, compromises the relay's ability to correct compute the actual system currents. This persists until much of the energization current transients reduce appreciably. To mitigate malfunction of this rather sensitive algorithm during reactor energization, a four (4) second time delay will be utilized to block the algorithm immediately following reactor energization. The

pickup time delay is based off of the typical X/R ratios of air core reactors (300 – 500). A higher pickup time delay is recommend for oil filled reactors as they typically have higher X/R ratios than air core reactors. Transient currents during reactor energization do approach nearly 95% of their steady state value within three (3) time constants. With an X/R ratio of 500, this comes down to about 3.98s, which is still under the four (4) seconds.

Several other ungrounded shunt reactor energization transients were played back in their respective relays and the algorithm (as implemented above) remained secure.

C. Solidly Grounded Bus Connected Reactor Failure

Xcel Energy practice does sometimes allow for installation of air core reactors on transmission buses. Shown in *figure 12* is a typical installation of a solidly grounded 25 MVAR shunt reactor on the 115kV bus. Two stacks of reactors are utilized per phase.

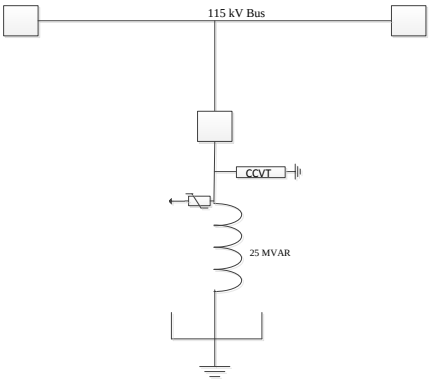

Figure 12: Grounded Wye Shunt Reactor

Existing protection

Primary reactor protection includes phase time overcurrent (51P) used for detection of phase and turn-to-turn faults. Ground time overcurrent (51G) is also utilized for providing protection against ground faults and excessive reactor imbalance. 51P is set to pick up at 130% of the reactor rating. 51G is set to pickup at 50% of the phase reactor rating. Restricted ground fault protection (87N), utilizing a time overcurrent, is also used to provide faster and more sensitive protection for ground faults in the reactor bank. Phase instantaneous overcurrent, set to 250% of the reactor rating, is used to provide backup protection for severe reactor faults.

On 4/14/2018, at 01:44:29, the reactor tripped and locked out. Field investigations indicated visible burn marks on the A-Phase reactor, shown in *figure 13*.

Figure 13: A-Phase faulty reactor following the 4/14/2018 event

Event records (*figure 14*) showed that this was a slow evolving turn-to-turn fault. 51P was the most sensitive element that picked up first. As the severity of the fault increased, the phase instantaneous overcurrent eventually picked up and tripped the reactor out. However, by the time the reactor was tripped out (at least 48 cycles after the fault was first detected), both reactor stacks had been damaged.

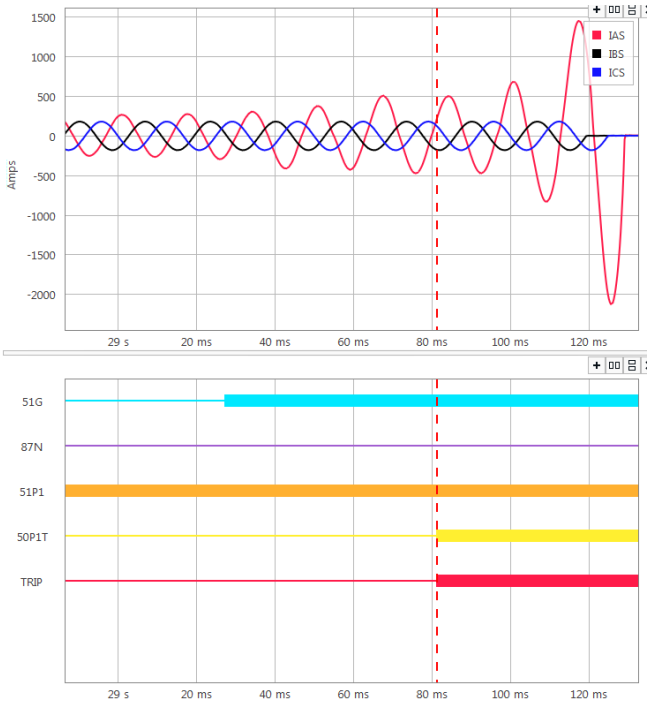

Figure 14: Relay records from the reactor relay following the 4/14/2018 event

Ground time overcurrent did see the fault but after several cycles.

Evaluation of the new algorithm

Event records were played back into the relay to evaluate the performance of the new algorithm. *Figure 15* shows that the new algorithm detects the fault and accurately identifies the faulted phase.

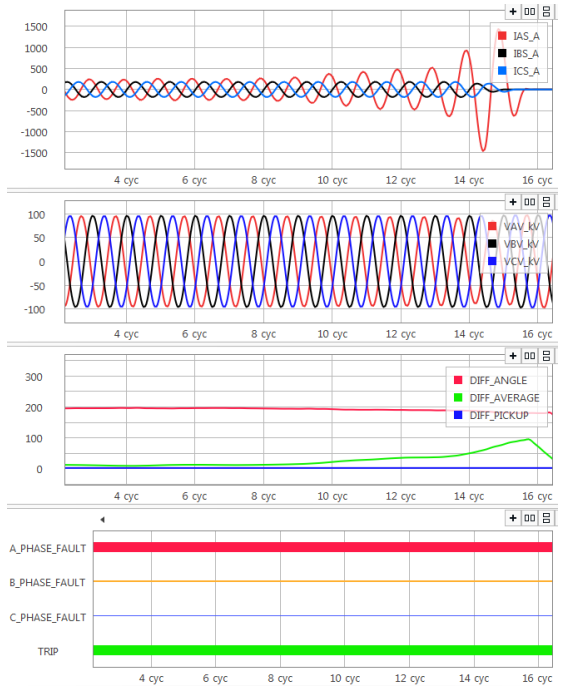

Figure 15: Relay records from the reactor relay following the 4/14/2018 event

Again, with a relay calculated Diff*average* value of 10% (in the low fault magnitude region), it's obvious that the fault might have gotten picked up and removed from the system much faster than the standard protection elements did. In this application, one reactor stack might have been saved. Therefore, had this algorithm been implemented in the relay at the time of the event, only one reactor stack may have needed replacement.

D. Evaluation of the Algorithm against Normal Grounded Reactor Energization

The faulted reactor was replaced and the new algorithm was evaluated against the energization transients. The energization time delay for blocking the algorithm was temporarily disabled for this test. *Figure 16* shows that algorithm remains stable despite some obvious energization transients that compromise the algorithm. The proposed energization time delay allows sufficient time for the transients to die.

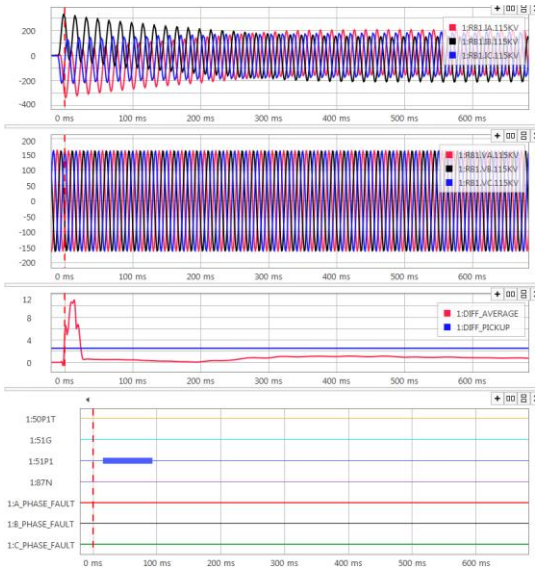

Figure 16: Evaluation of the performance of the new algorithm during grounded shunt reactor energization

E. Stability of the Algorithm against External Faults

By design, as shown in *figures 2 & 3*, the algorithm gets blocked when any of the phase voltages drops below 80% of their nominal value. For this paper, the algorithm has purposefully been enabled to demonstrate its superior and secure performance even during external fault conditions.

Solidly Grounded Reactors

The security and performance of the algorithm was also assessed against external faults. *Figure 17* shows how the algorithm performed during an external A-C phase to phase fault, 5.5 mile from the substation. Transients during line reclosing are also evaluated.

Figure 17: Evaluation of the performance of the new algorithm, implemented on the grounded shunt reactor, during an external line-to-line fault

Diff*average* only momentarily (< 2cycles) changed or exceeded Diff*pickup* at the fault inception, and reclosing transient. This demonstrates that the 5.0 cycle used to permit ride through during such transients is adequate.

Figure 18 further demonstrates that the algorithm is still secure even during an external single line-to-ground fault, 7.5 miles from the substation.

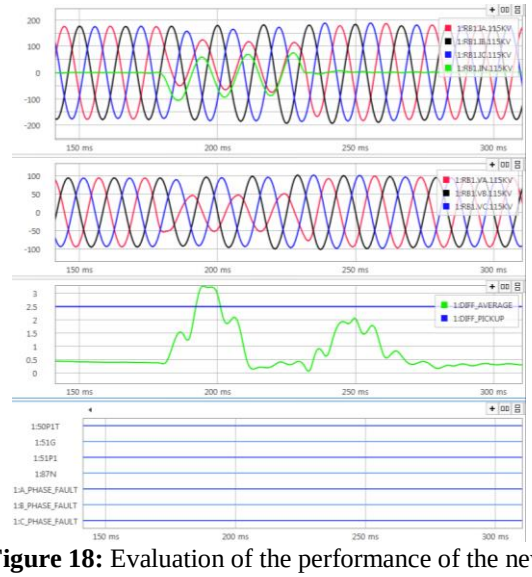

Figure 18: Evaluation of the performance of the new algorithm, implemented on the grounded shunt reactor, during an external line-to-ground fault

Ungrounded Reactors

Since no event records are typically triggered for external faults on transformer tertiary connected reactor relays, PSCAD software was used to create a detailed model of the tertiary reactor in *figure 3*. This was then used to simulate external faults. The comtrade files that were created were played back into the relay to evaluate the performance of the algorithm. *Figures 19 and 20* do show that the algorithm remains stable during A-G, and B-C bus faults on the 115kV bus.

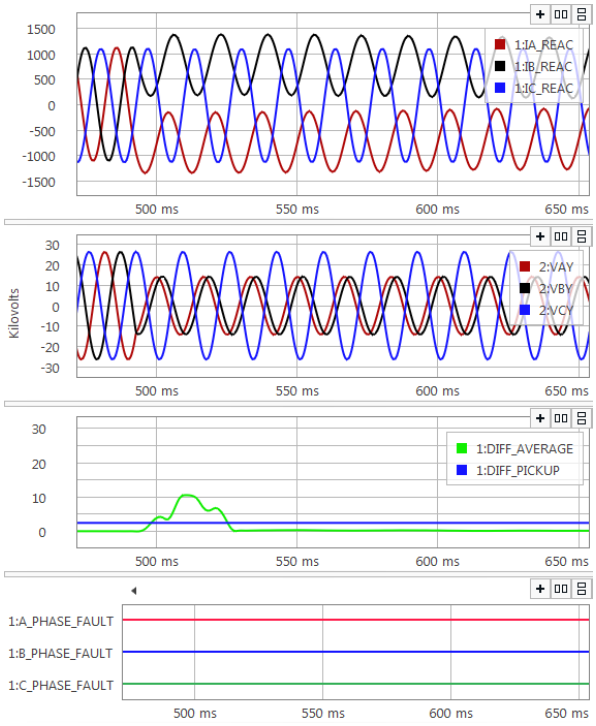

Figure 19: Evaluation of the performance of the new algorithm, implemented on the ungrounded shunt reactor, during an external line-to-ground fault

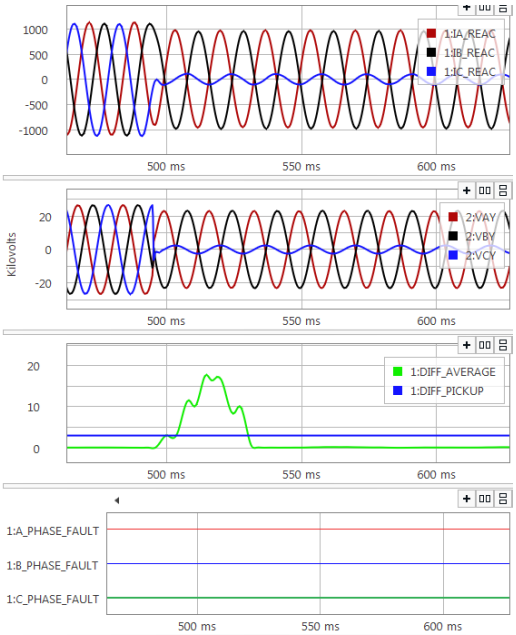

Figure 20: Evaluation of the performance of the new algorithm, implemented on the ungrounded shunt reactor, during an external line-to-line fault

Figures 17-20 demonstrate that the security of the algorithm remains uncompromised during external faults

F. De-energization of Mutually Coupled Shunt Compensated Line

Figure 21 shows the configuration of the circuit under study. The figure comprises two parallel, 75 mile lines that are mutually coupled together with one of them having a 50 MVAR shunt compensation reactor (oil filled) connected at its line end.

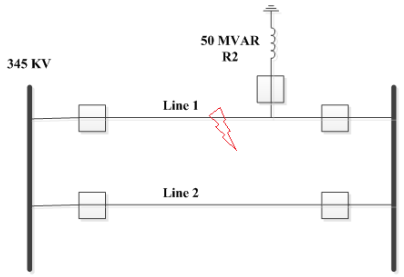

Figure 21: Double Circuited 345kV lines

A single line-to-ground fault occurred on the shunt compensated line; protection tripped line end breakers and kept the line out. Capacitive coupling between the energized line and the de-energized shunt compensated line sustained significant transient oscillation that saw the reactor trip out via the negative sequence time overcurrent element (set to 20% of the reactor rating). Comtrade files from the shunt reactor relays were obtained and played back in the relay, with voltage supervision disabled (otherwise, it would have blocked the algorithm), to evaluate the algorithm's performance. *Figure 22* shows the reactor transient voltages and currents, more than eighty (80) cycles after the line #1 tripped out.

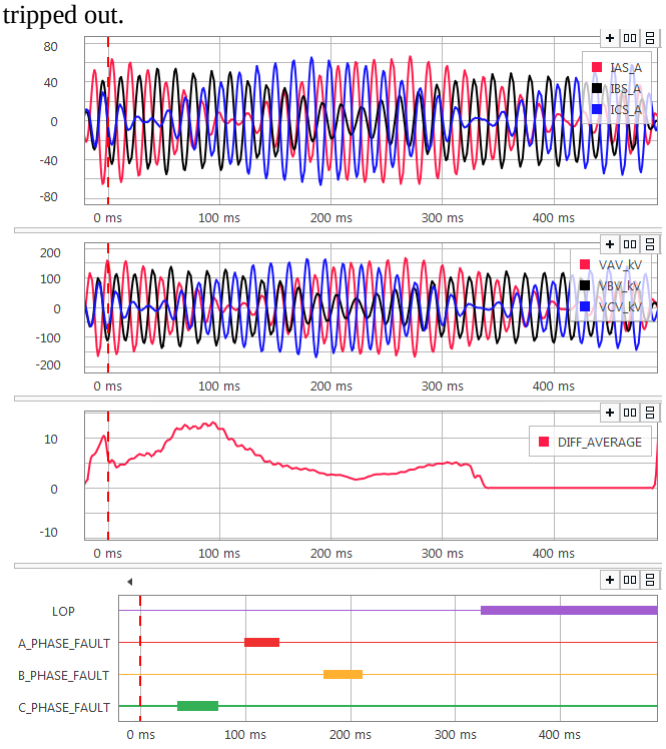

Figure 22: Evaluation of the performance of the new algorithm due transients on mutually couple shunt compensated line

The transient sub-harmonic oscillations do compromise the algorithm leading to Diff$average$ that is significantly higher than the set Diff$pickup$ value.

Failure of the algorithm is attributed to the sub-harmonic resonant oscillations which impact the relays' ability to correctly calculate voltage and current sequence components, on which the algorithm is based, at 60 Hz. To mitigate such a mis-operation without compromising the algorithm's sensitivity, line breaker status is utilized to supervise the algorithm. In other words, the algorithm is inoperable if the line end breaker is closed; the line is energized with a good 60Hz source.

V. CONCLUSIONS

This paper has demonstrated the field implementation of the algorithm, discussed in [3], for sensitively detecting turn-turn faults in air core reactors and identifying the faulted reactor simultaneously. Sensitive and fast identification of faults ensures that they are quickly removed from the system. This minimizes fire hazards in the substation. Identification of the faulted phase also minimizes time and resources spent on fault location investigation. And lastly, for all applications involving more than one reactor stack per phase, quick fault identification may help minimize damage and the number of reactors that may need replacement. This helps cut down on the operations and maintenance costs.

References

[1] IEEE Guide for the Protection of Shunt Reactors, ANSI/IEEE C37.109-1988

[2] Bogdan Kasztenny, Normann Fischer, Hector J. Altuve, "Negative-Sequence Differential Protection – Principles, Sensitivity, and Security", 68th Annual Conference for Protective Relay Engineers, March 2015, Texas A&M University

[3] Sarasij Das, Tarlochan Sidhu, Mohammed Reza Dadash, Zhiying Zhang. A Novel Method for Turn to Turn Fault Detection in Shunt Reactors. *70th Annual Conference for Protective Relay Engineers*, April 2017, Texas A&M University

IEEE Standard Requirements, Terminology, and test Code for Shunt Reactors Rated Over 500 kVA, IEEE Std C57.21-200

[4] Bogdan Kasztenny, Normann Fischer, Douglas Taylor, Tejasvi Prakash, Jeevan Jalli "Do CTs Like DC? Performance of Current Transformers With Geomagnetically Induced Currents", 69th Annual Conference for Protective Relay Engineers, April 2016, Texas A&M University

Biographies

Paul Nyombi is a System Protection Engineer with Xcel Energy in Minneapolis, MN where he works with transmission system protective relays and their settings. He has over five (5) years of experience as a relay protection engineer. He is a professional engineer in the state of Minnesota. Paul holds a BSc. in Electrical Engineering and Computer Science, and MSc. in Electrical Engineering from St. Thomas University, St. Paul, Minnesota.

Pratap G Mysore, Founder –Pratap Consulting Services, has over forty years of experience in the power industry. He is a registered professional engineer in the state of Minnesota and a senior member of IEEE.

He is a member of IEEE Power Systems Relaying and Control Committee and member of T&D Capacitor Subcommittee. He has taught protection courses at the University of Minnesota, Georgia Tech Relay School and developed media modules for the Consortium of Universities for Sustainable Power (CUSP),

Pratap has authored several papers and presented tutorials and papers at MIPSYCON and at all relay conferences. He is a member of the WPRC planning committee.

Zhiying Zhang received his B.Sc. and M.Sc. degrees from North China Electric Power University and a Ph.D. degree from the University of Manitoba, Canada, all in Electrical Engineering. He has over thirty years of working experience with Electric utilities and with relay manufactures in various technical positions. Since 2007 he has been with General Electric, and currently holds the position of principal applications engineer at GE Grid Solutions in Markham, Ontario. Zhiying is a registered professional engineer in the province of Ontario, and a senior member of IEEE.

Appendix

Annex A

A sample example considering a 50 MVAR solidly grounded reactor, installed on a bus with short circuit strength of 1000MVA, is given for illustration in *figure A.1*.

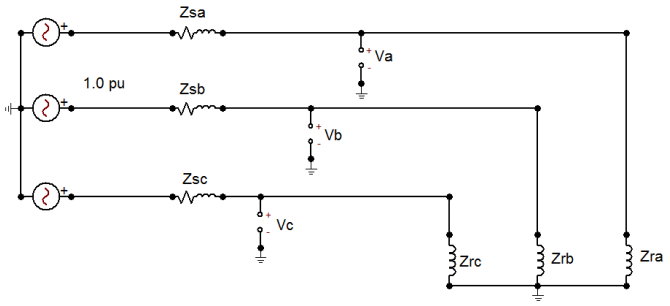

Figure A.1: Simplified Circuit of a Solidly Grounded Reactor

The source and reactor per unit impedances on 100MVA are calculated as,

Source impedance, Z_{src} (Zsa, Zsb, Zsc) = 0.1 p.u
And reactor impedance, Z_{reac} (Zra, Zrb, Zrc) = 2.0 p.u

A. Consider a 5% decrease in the A-phase reactor impedance

Substituting, Z_{reac}, in equation (3), gives the normalized negative sequence current as:

$$\frac{I_2}{I_1} = \frac{1.0526V_a + a^2V_b + aV_c}{1.0526V_a + aV_b + a^2V_c} = \frac{0.0526V_a + (V_a + a^2V_b + aV_c)}{0.0526V_a + (V_a + aV_b + a^2V_c)}$$

Where, V_a, V_b, and V_c are bus voltages as measured at the reactor terminal. V_n is zero for a solidly grounded reactor as used in this example.

$$\frac{I_2}{I_1} = \frac{0.0526V_a + 3V_2}{0.0526V_a + 3V_1} \quad \text{(A.2)}$$

The reactor terminal voltages are computed as:

$$V_a = \frac{1}{Z_{src} + 0.05Z_{reac}} \times 1.0\ p.u = \frac{1}{0.1 + 0.05 \times 2.0} \times 1.0\ p.u = 0.95\angle 0°\ p.u$$

$$V_b = \frac{1}{Z_{src} + Z_{reac}} \times 1.0\ p.u = \frac{1}{0.1 + 2.0} \times 1.0\ p.u = 0.952\angle -120°\ p.u$$

$$V_c = \frac{1}{Z_{src} + Z_{reac}} \times 1.0\ p.u = \frac{1}{0.1 + 2.0} \times 1.0\ p.u = 0.952\angle 120°\ p.u$$

From the reactor terminal voltages computed above, $3V_1$, and $3V_2$ are calculated as $2.854\angle 0°\ p.u$, and $-0.002\angle 0°\ p.u$ respectively.

This gives negative sequence normalized voltage as:

$$\frac{V_2}{V_1} = 0.0007\angle 180°\ p.u \quad \text{(A.3)}$$

Substituting, $3V_1$, and $3V_2$ in *equation (A.2),*

$$\frac{I_2}{I_1} = \frac{0.0526 \times 0.95\angle 0° - 0.002\angle 0°}{0.0526 \times 0.95\angle 0° + 2.854\angle 0°} = 0.016519\angle 0°$$

From the calculated, $\frac{V_2}{V_1}$, and $\frac{I_2}{I_1}$ values, Diff$pickup$ for shorting in the A-phase reactor is given as:

$$\text{Diff}pickup = 0.0007\angle 180° - 0.016519\angle 0° \cong 0.017219\angle 180°$$

B. Consider a 5% decrease in the B-phase reactor impedance

From equation (3), the normalized negative sequence current is computed as:

$$\frac{I_2}{I_1} = \frac{0.0526 \times a^2V_b + 3V_2}{0.0526 \times aV_b + 3V_1} \quad \text{(A.4)}$$

$3V_1$, and $3V_2$ are computed from the reactor terminal voltages, are given as $2.854\angle 0°\ p.u$, and $-0.002\angle 120°\ p.u$ respectively.

Negative sequence voltage normalization is computed as:

$$\frac{V_2}{V_1} = -0.0007\angle 120°\ p.u \quad \text{(A.5)}$$

Substituting, $3V_1$, and $3V_2$ in *equation (A.4),*

$$\frac{I_2}{I_1} = 0.016519\angle 120°$$

From the calculated, $\frac{V_2}{V_1}$, and $\frac{I_2}{I_1}$ values, Diff$pickup$ for shorting in the B-phase reactor is given as:

$$\text{Diff}pickup = -0.0007\angle 120° - 0.016519\angle 120° \cong 0.017219\angle -60°$$

C. Consider a 5% decrease in the C-phase reactor impedance

$\frac{V_2}{V_1}$, and $\frac{I_2}{I_1}$ values, derived similarly as shown above, are used to compute Diff$pickup$ for shorting in the C-phase reactor.

$$\text{Diff}pickup = -0.0007\angle 240° - 0.016519\angle 240° \cong 0.017219\angle 60°$$

Calculations above demonstrate that with 5% decrease in the faulted reactor impedance, the magnitude of the calculated percent differential quantity between $\frac{V_2}{V_1}$, and $\frac{I_2}{I_1}$ is around 1.72%. The phasor of the calculated differential values correctly identifies the faulted phase as given in *table 1[3]*.

Annex B

```
#TURN TO TURN FAULT DETECTION
#SUPRVISE ALGORITHM
LogicVar1 = 593P #VOLTAGE IN ALL THREE PHASES MUST BE ABOVE 80%
Latch5 = LogicVar1
Latch5_PU = 0.0
Latch5_DO = 2.0

LogicVar2 = IN201 #LOAD CURRENT MUST BE PRESENT (BREAKER CLOSED)

Latch1 = LogicVar2 # BKR CLOSED
Latch1_PU = 240.0
Latch1_DO = 0.0

LogicVar20 = (V0_Mag > 0.3*V1_Mag) # NO GROUND FAULT ON TERTIARY BUS
Latch4 = LogicVar20 # BKR CLOSED
Latch4_PU = 2.0
Latch4_DO = 0.0

LogicVar21 = NOT (LOP OR Latch4Q) AND (Latch5Q AND Latch1Q) # NO GROUND FAULT OR LOP ON TERTIARY BUS

#V2/V1 PHASOR CALCULATIONS
LogicNum1 = (V2_Mag/ V1_Mag) * LogicVar21 #V2/V1 MAGINTUDE
LogicNum2 = (V2_Angle - V1_Angle) * LogicVar21 #V2/V1 ANGLE

#V2/V1 CALCULATIONS

#CONVERSSION OF V2/V1 TO RECTANGULAR FORM
LogicNum3 = 100.0 * LogicNum1 * COS(LogicNum2) #PERCENT V2/V1 REAL COMPONENT
LogicNum4 = 100.0 * LogicNum1 * SIN(LogicNum2) #PERCENT V2/V1 IMAGINARY COMPONENT

#I2/I1 PHASOR CALCULATIONS
LogicNum5 = (I2_Mag / I1_Mag) * LogicVar21 #I2/I1 MAGINTUDE
LogicNum6 = (I2_Angle - I1_Angle) * LogicVar21 #I2/I1 ANGLE

#CONVERSSION OF I2/I1 TO RECTANGULAR FORM
LogicNum7 = 100.0 * LogicNum5 * COS(LogicNum6) #IPERCENT I2/I1 REAL COMPONENT
LogicNum8 = 100.0 * LogicNum5 * SIN(LogicNum6) #IPERCENT I2/I1 IMAGINARY COMPONENT

#VOLTAGE (V2/V1) - CURRENT (I2/I1)
LogicNum9 = LogicNum3 - LogicNum7 #REAL COMPONENT
LogicNum10 = LogicNum4 - LogicNum8 #IMAGINARY COMPONENT

#REGISTER ARRAY OF THE PREVIOUS 8, (V2/V1 - I2/I1) VALUES WITH FIFO

LogicNum25 = LogicNum23
LogicNum26 = LogicNum24
LogicNum23 = LogicNum21
LogicNum24 = LogicNum22
LogicNum21 = LogicNum19
LogicNum22 = LogicNum20
LogicNum19 = LogicNum17
LogicNum20 = LogicNum18
LogicNum17 = LogicNum15
LogicNum18 = LogicNum16
LogicNum15 = LogicNum13
LogicNum16 = LogicNum14
LogicNum13 = LogicNum11
LogicNum14 = LogicNum12
LogicNum11 = LogicNum9 #REAL COMPONENT
LogicNum12 = LogicNum10 #IMAGINARY COMPONENT
```

```
#COMPUTE AVERAGE DIFF
LogicNum27 = (LogicNum11 + LogicNum13 + LogicNum15 + LogicNum17 + LogicNum19 + LogicNum21 + LogicNum23 +
LogicNum25) / 8.0 #AVERAGE REAL COMPONENT
LogicNum28 = (LogicNum12 + LogicNum14 + LogicNum16 + LogicNum18 + LogicNum20 + LogicNum22 + LogicNum24 +
LogicNum26) / 8.0 #AVERAGE IMAGINARY COMPONENT


#CONVERT AVERAGE DIFF BACK TO POLAR FORM
LogicNum29 = SQRT((LogicNum27 * LogicNum27) + (LogicNum28 * LogicNum28)) #MAGINTUDE

#FAULT DETERMINATION

LogicNum30 = 3.0 #DIFF_ PICKUP
LogicVar3 = (LogicNum29 > LogicNum30) #TURN TO TURN FAULT DETECTED

Latch2 = LogicVar3 #PICKUP TIME DELAY FOR ALGORITHM
Latch2_PU = 10.0
Latch2_DO = 0.0

Latch3 = LogicVar3 #BY-PASS TIMER
Latch3_PU = 5.0
Latch3_DO = 0.0

LogicVar4 = (87HG1 OR 87TG1 OR 51P1 OR 51Q1) #PICKUP OF OTHER PROTECTION ELEMENTS

#CALCULATIONS FOR DIFF_AVERAGE ANGLE
LogicVar5 = (LogicNum28 > 0.0) AND (LogicNum27 > 0.0) AND LogicVar3 #QUADRIT 1
LogicVar6 = (LogicNum28 > 0.0) AND (LogicNum27 < 0.0) AND LogicVar3 #QUADRIT 2
LogicVar7 = (LogicNum28 < 0.0) AND (LogicNum27 < 0.0) AND LogicVar3 #QUADRIT 3
LogicVar8 = (LogicNum28 < 0.0) AND (LogicNum27 > 0.0) AND LogicVar3 #QUADRIT 4
LogicNum31 = (ACOS(LogicNum27/ LogicNum29) * LogicVar5) + ((180.0 - ASIN(LogicNum28/ LogicNum29)) *
LogicVar6) #QUADRIT 1 OR 2 ANGLE
LogicNum32 = ((180.0 + ACOS(-1.0 * LogicNum27/ LogicNum29)) * LogicVar7) + ((360.0 -
ACOS(LogicNum27/LogicNum29)) * LogicVar8) #QUADRIT 3 OR 4 ANGLE
LogicNum33 = (LogicNum31 + LogicNum32) #ANGLE

#TRIP
LogicVar9 = (Latch2Q OR Latch3Q AND LogicVar4)

#FAULTED PHASE IDENTIFICATION
LogicVar10 = (150.0 <= LogicNum33) AND (LogicNum33 <= 210.0) AND LogicVar9 #TURN TO TURN FAULT IN A-PHASE
LogicVar11 = (270.0 <= LogicNum33) AND (LogicNum33 <= 330.0) AND LogicVar9 #TURN TO TURN FAULT IN B-PHASE
LogicVar12 = (30.0 <= LogicNum33) AND (LogicNum33 <= 90.0) AND LogicVar9 #TURN TO TURN FAULT IN C-PHASE
```